

Electronic Supporting Information.

**Multinuclear ( $^{67}\text{Zn}$ ,  $^{119}\text{Sn}$  and  $^{65}\text{Cu}$ ) NMR spectroscopy, an ideal technique to probe the cationic ordering in  $\text{Cu}_2\text{ZnSnS}_4$  photovoltaic materials**

**Léo Choubrac,\* Michaël Paris, Alain Lafond,\* Catherine Guillot-Deudon, Xavier Rocquefelte and Stephane Jobic**

Institut des Matériaux Jean Rouxel (IMN), Université de Nantes, CNRS  
2, rue de la Houssinière, BP 32229, 44322 Nantes cedex 03, France

*Corresponding authors:* [leo.choubrac@cnrs-imn.fr](mailto:leo.choubrac@cnrs-imn.fr) & [alain.lafond@cnrs-imn.fr](mailto:alain.lafond@cnrs-imn.fr)

## Experimental details

### Composition analyses

The composition of the stoichiometric precursor was measured by electron probe micro-analysis (EPMA) with the operating conditions: accelerating voltage 20 kV, current 20 nA, 2  $\mu\text{m}$  beam diameter; standards (element, emission line, counting time for one spot analysis): Cu metal (Cu K $\alpha$ , 10 s), ZnS (Zn K $\alpha$ , 10 s), SnO<sub>2</sub> (Sn L $\alpha$ , 20 s), FeS<sub>2</sub> (S K $\alpha$ , 20 s).

The compositions of the 4 annealed samples (VS, S, F and VF, see text) have been checked by EDX analysis under the operating conditions: accelerating voltage 20 kV, current 1.5 nA. A stoichiometric Cu<sub>2</sub>ZnSnS<sub>4</sub> was used as a internal standard (Cu K $\alpha$ , Zn K $\alpha$ , Sn L $\alpha$ , S K $\alpha$ , 10<sup>6</sup> cts/spectrum). For each samples, ten spot analyses were performed in distinct areas. No significant difference between the four samples was evidenced. Data are given in table S2.

### Powder X-ray diffraction

The X-ray powder diffraction patterns of all CZTS samples have been collected on Bruker D8-diffractometer in Bragg-Brentano geometry with the monochromatized Cu (K $\alpha$ 1) radiation and a LynxEye detector.

### NMR

The <sup>119</sup>Sn, <sup>65</sup>Cu and <sup>67</sup>Zn NMR spectra were acquired on two Bruker Avance III 300 and 500 MHz spectrometers with 2.5 mm and 4mm CP-MAS probes. Rotors were spun at 14 kHz, 30 kHz and 10 kHz for <sup>119</sup>Sn, <sup>65</sup>Cu and <sup>67</sup>Zn MAS spectra, respectively. Additional <sup>65</sup>Cu spectra were acquired under static (no MAS) conditions. Recycle time were 120s for <sup>119</sup>Sn and 1s for <sup>65</sup>Cu. For <sup>67</sup>Zn, we used 2s for the VS-CZTS sample and 1s for the VF-CZTS one. To obtain an absorption mode only lineshape, both <sup>119</sup>Sn and <sup>65</sup>Cu spectra were obtained using a full shifted echo acquisition ( $\theta - \tau - 2\theta - \text{acq}$ ). For the <sup>119</sup>Sn spectra,  $\tau$  was set to 1.9 ms and  $\theta$  to  $\pi/2$  for a RF field of 80 kHz. For the <sup>65</sup>Cu MAS spectrum, we used  $\theta = \pi/6$  for a RF field of 60 kHz and  $\tau$  ranging between 3.3 ms (VS-CZTS) and 1.0 ms (VF-CZTS). For the static <sup>65</sup>Cu spectra, we used  $\theta = \pi/10$  for a RF field of 35 kHz and  $\tau = 1.2$  ms. <sup>67</sup>Zn MAS spectra were obtained with a rotor synchronized Hahn echo sequence ( $\pi/6 - \tau - \pi/3 - \tau - \text{acq}$ ) with  $\tau$  equals one rotor period. Spectra were referenced at 0 ppm against solid state CuCl for <sup>65</sup>Cu and a Zn(NO<sub>3</sub>)<sub>2</sub>(aq) solution for <sup>67</sup>Zn. Finally, <sup>119</sup>Sn spectra were referenced to Me<sub>4</sub>Sn using Ph<sub>4</sub>Sn as a secondary reference (-121.15 ppm). The spectral decompositions were conducted with the help of the “dmfit” freeware package.<sup>1</sup>

### Ab initio calculations

DFT calculations were performed using the VASP (Vienna Ab initio simulation Package)<sup>2</sup> code with the PBE functional for exchange and correlation.<sup>3</sup> EFG were calculated using the PAW method.<sup>4</sup> To achieve convergence of the EFG calculations, the plane wave basis sets were expanded to an energy cut-off of 500 eV and a 4x4x2 Monkhorst-Pack<sup>5</sup> k-points grid was used. The crystallographic structure determined by single crystal XRD (table SI-T1) was used without any geometry optimization prior to calculations. We use  $Q(^{65}\text{Cu}) = -20.4 \text{ fm}^2$  and  $Q(^{67}\text{Zn}) = 15.0 \text{ fm}^2$ .<sup>6</sup> Calculations were carried out only on the long range ordered structure.

## Spectral decomposition of the $^{65}\text{Cu}$ NMR spectrum of the VS-CZTS compound

The Figure S5 shows the two individual lines (W and N) of the spectral decomposition of the  $^{65}\text{Cu}$  spectrum acquired under static condition on a 500 MHz spectrometer (11.75 T). Although the overall features of the spectrum is fully reproduced, additional arguments in favor of the decomposition can be given by the use of another magnetic field strength ( $B_0$ ). Indeed, changing the magnetic field modifies the lines shapes as both the chemical shift interaction (proportional to  $B_0$ ) and the quadrupolar interaction to a second order approximation (proportional to  $1/B_0$ ) depend on the static magnetic field. The figure S6 presents the  $^{65}\text{Cu}$  spectrum acquired on a 300 MHz spectrometer (7.05 T) (all others conditions identical). The spectral decomposition of this spectrum performed with the same parameters values as the ones used on figure S5 is very successful. Further supported by the MAS spectrum shown on the figure S7, this gives high confidence in the  $C_Q, \eta, \delta_{iso}, \delta_{aniso}, \eta$  and  $\beta$  values proposed here.

## Discussion about the secondary phases

The presence of secondary phases in CZTS thin films is an important issue for the energy conversion efficiency of the corresponding solar cells. Thus, we have paid attention to be sure that our samples do not contain any impurities.

A few percents of secondary phases such as SnS, SnS<sub>2</sub>, Sn<sub>2</sub>S<sub>3</sub>, ZnS would easily be distinguishable on the  $^{119}\text{Sn}$  or  $^{67}\text{Zn}$  NMR spectra since they exhibit very sharp signals far away from the CZTS ones.<sup>8,9</sup> On the other hand, copper sulfides are often non-stoichiometric, as Cu<sub>2-x</sub>S in which a part of copper atoms are at +II valence state. The presence of these paramagnetic atoms makes these copper sulfides almost invisible on the  $^{65}\text{Cu}$  NMR spectra or could prevent any NMR measurements if the concentration was too large. The last envisioned secondary phase is Cu<sub>2</sub>SnS<sub>3</sub> for which we have estimated the quadrupolar constants related to the two copper sites (space group: Cc) using the same theoretical methodology (PBE calculations using VASP). In contrast to CZTS the two copper tetrahedral sites in this compound are strongly distorted. As a consequence, the  $C_Q$  and  $\eta$  values are expected to be large, which is confirmed by the DFT analysis leading to  $C_Q(\text{Cu1}) = -19.9$  MHz,  $\eta(\text{Cu1}) = 0.646$  and  $C_Q(\text{Cu2}) = +12.8$  MHz et  $\eta(\text{Cu2}) = 0.971$ . These values are far away from both the observed and the calculated ones for the kesterite Cu<sub>2</sub>ZnSnS<sub>4</sub>. On the other hand, it is expected from unpublished results on related compounds that the corresponding  $^{119}\text{Sn}$  spectrum should consist of a single narrow line well distinct from that of CZTS.

From PXRD, EDX and NMR investigations, we can definitely conclude that the studied samples are only composed of the stoichiometric Cu<sub>2</sub>ZnSnS<sub>4</sub> compound.

**Table S1.** Atomic positions and bond angles in the kesterite structure of  $\text{Cu}_2\text{ZnSnS}_4$  (from reference <sup>7</sup>)

<i>I</i> -4 position	atom	sof	x	y	z	M-S bond length (Å)	angle A(°)	angle B(°)	angle variance (° <sup>2</sup> )
2a	Cu	1	0	0	0	2.332	110.8	106.8	4.27
2b	Sn	1	0	0	0.5	2.411	109.41	109.60	0.01
2c	Cu	1	0	0.5	0.25	2.333	111.1	108.7	1.54
2d	Zn	1	0	0.5	0.75	2.330	111.0	108.7	1.41
8g	S	1	0.7562(2)	0.2434(2)	0.12821(6)	-	-	-	-

Space group: *I*-4, cell parameters  $a=5.4344(15)$  Å and  $c=10.8382(6)$  Å. Angles A and B have multiplicity of 4 and 2 respectively.

**Table S2.** Atomic compositions and unit cell parameters of the studied samples.

Sample	Cu (at %)	Zn (at %)	Sn (at %)	S (at %)	a (Å)	c(Å)	Cell volume (Å <sup>3</sup> )
VS	24.57(12)	12.65(13)	12.68(7)	50.11(15)	5.4334(1)	10.8325(2)	319.80(1)
S	24.74(22)	12.65(20)	12.61(6)	50.00(16)	5.4342(2)	10.8350(3)	319.96(2)
F	24.85(21)	12.60(22)	12.57(8)	49.99(15)	5.4341(1)	10.8407(2)	320.12(1)
VF	24.76(22)	12.58(15)	12.68(4)	49.98(16)	5.4336(1)	10.8421(3)	320.10(2)

ESD are given in parenthesis

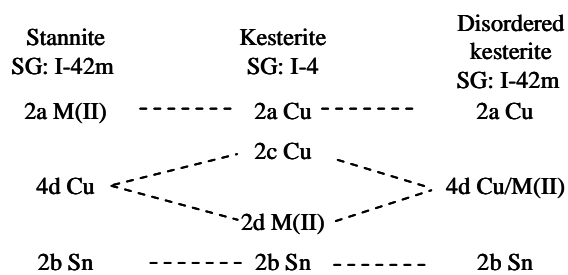


**Figure S1.** Relationship between the crystallographic positions of cations in stannite, kesterite, and disordered-kesterite structures

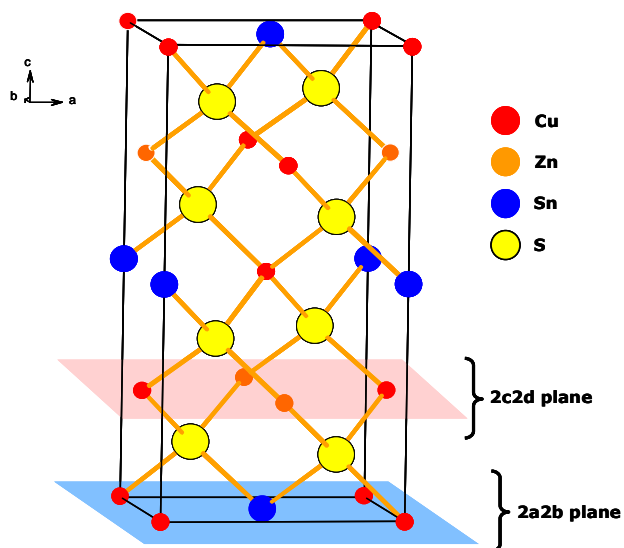


**Figure S2.** Representation of the KS-Structure

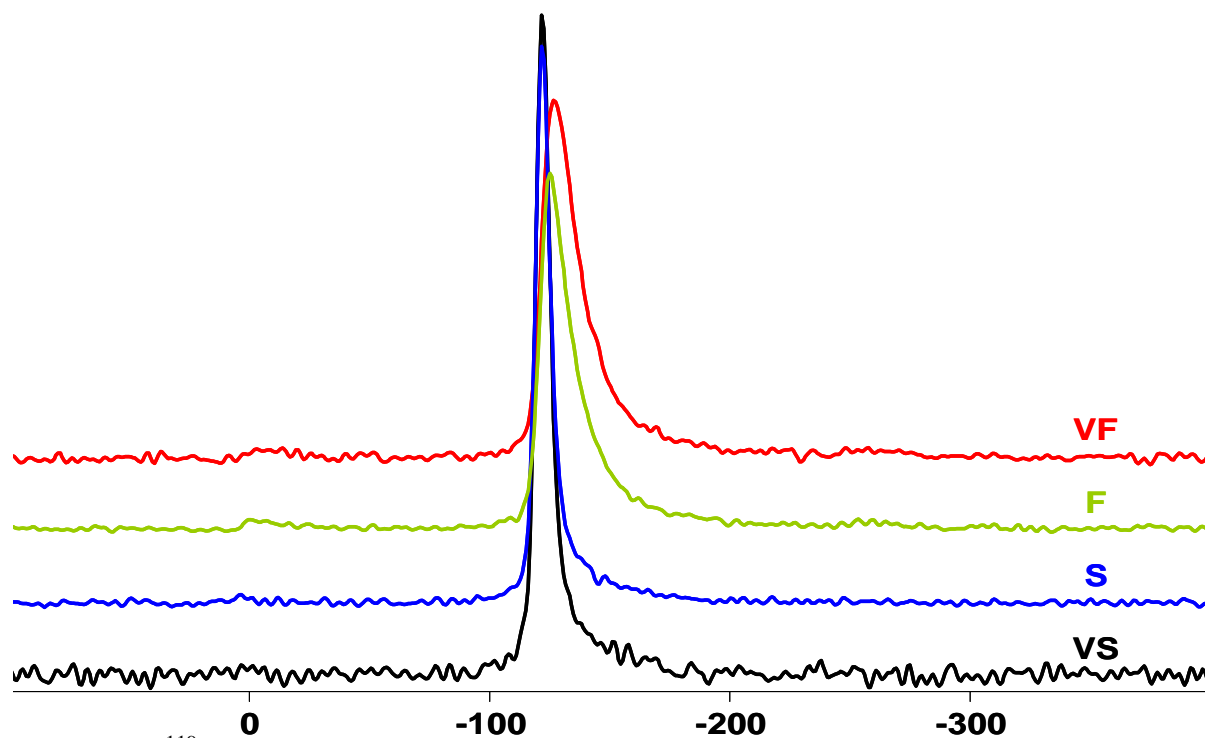


**Figure S3.**  $^{119}\text{Sn}$  full shifted echo NMR spectra of the four compounds acquired under MAS (14kHz) condition on a 300MHz spectrometer (7.05T).

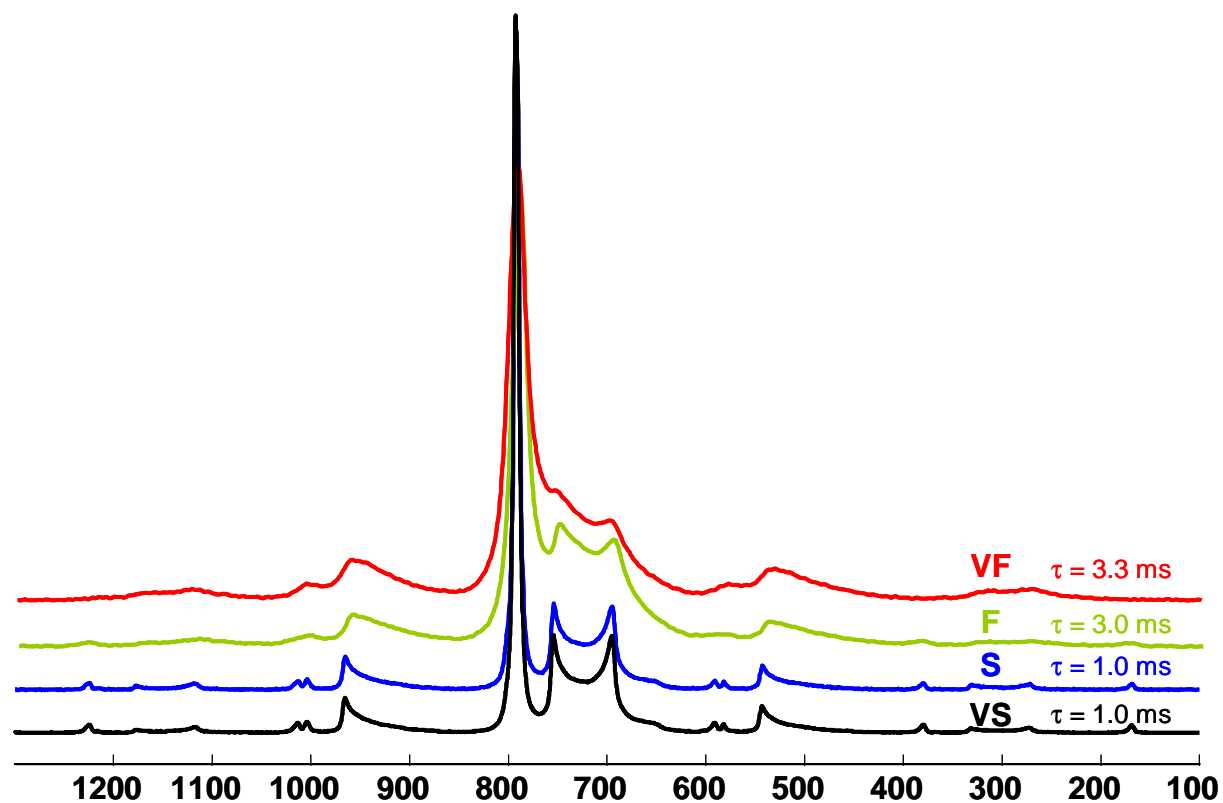


**Figure S4.**  $^{65}\text{Cu}$  full shifted echo NMR spectra of the four compounds acquired under MAS (30kHz) condition on a 500MHz spectrometer (11.75T).

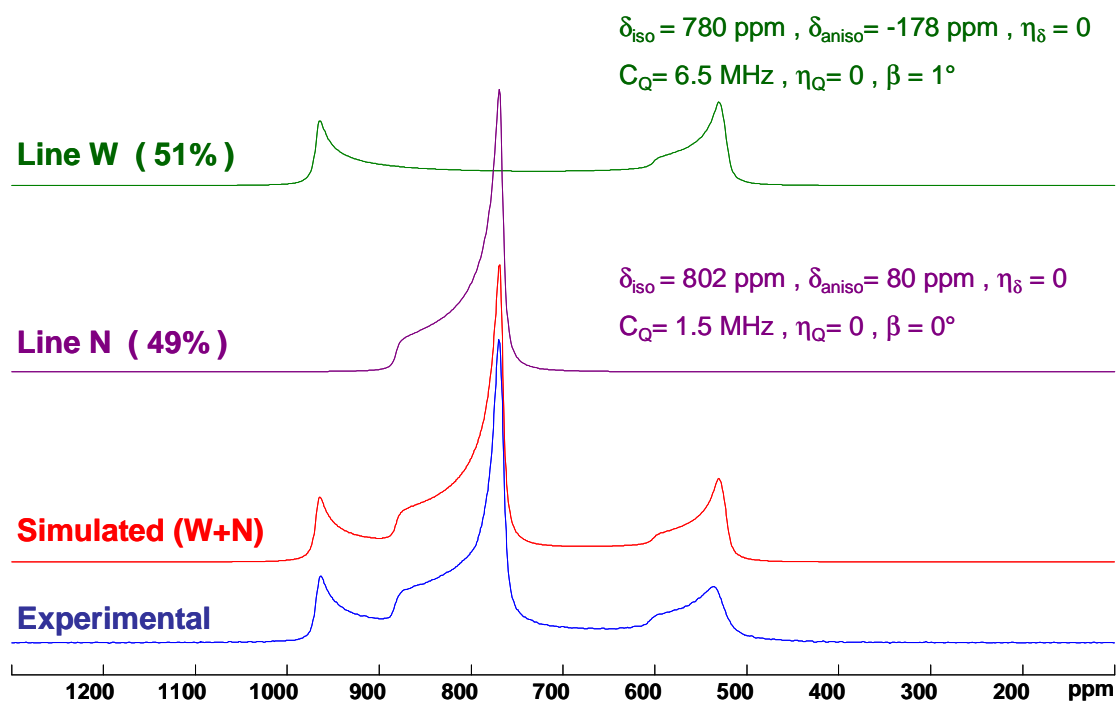


**Figure S5.** Spectral decomposition of the  $^{65}\text{Cu}$  full shifted echo NMR spectrum of the VS-CZTS compound acquired under static condition on a 500 MHz spectrometer (11.75 T).

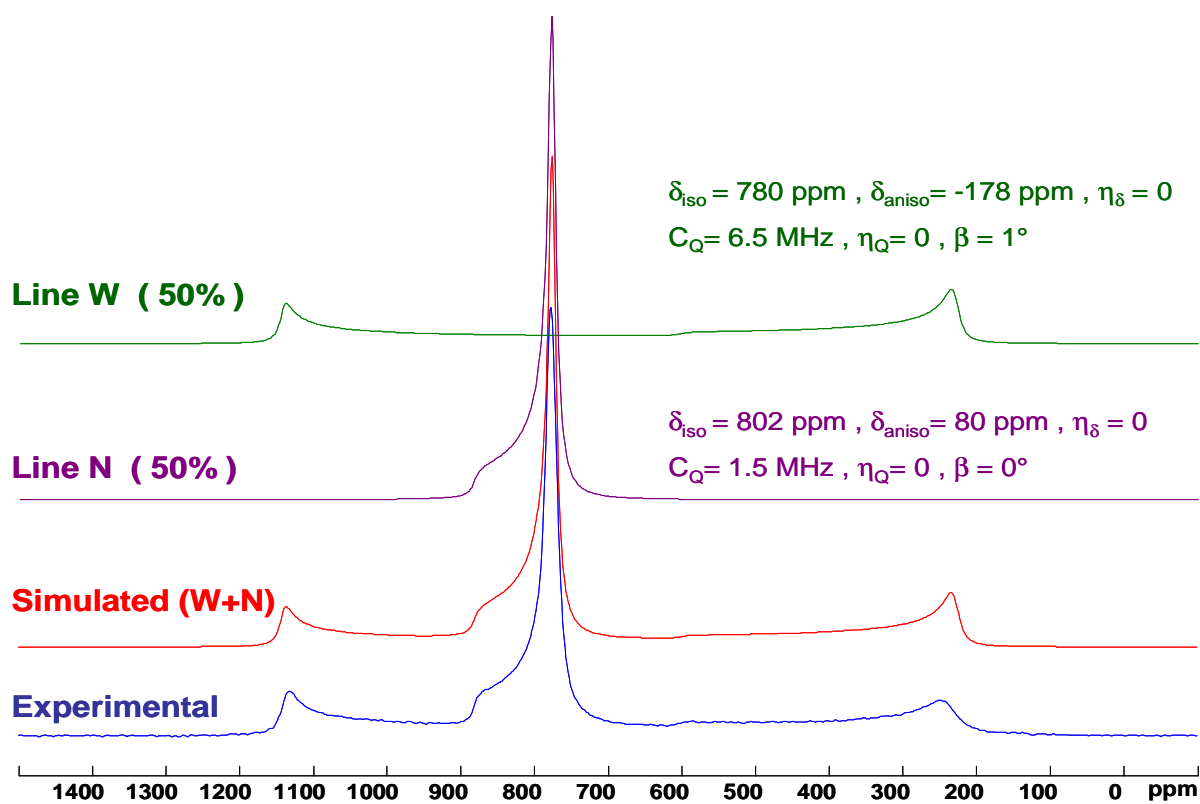


**Figure S6.** Spectral decomposition of the  $^{65}\text{Cu}$  full shifted echo NMR spectrum of the VS-CZTS compound acquired under static condition on a 300 MHz spectrometer (7.05 T)

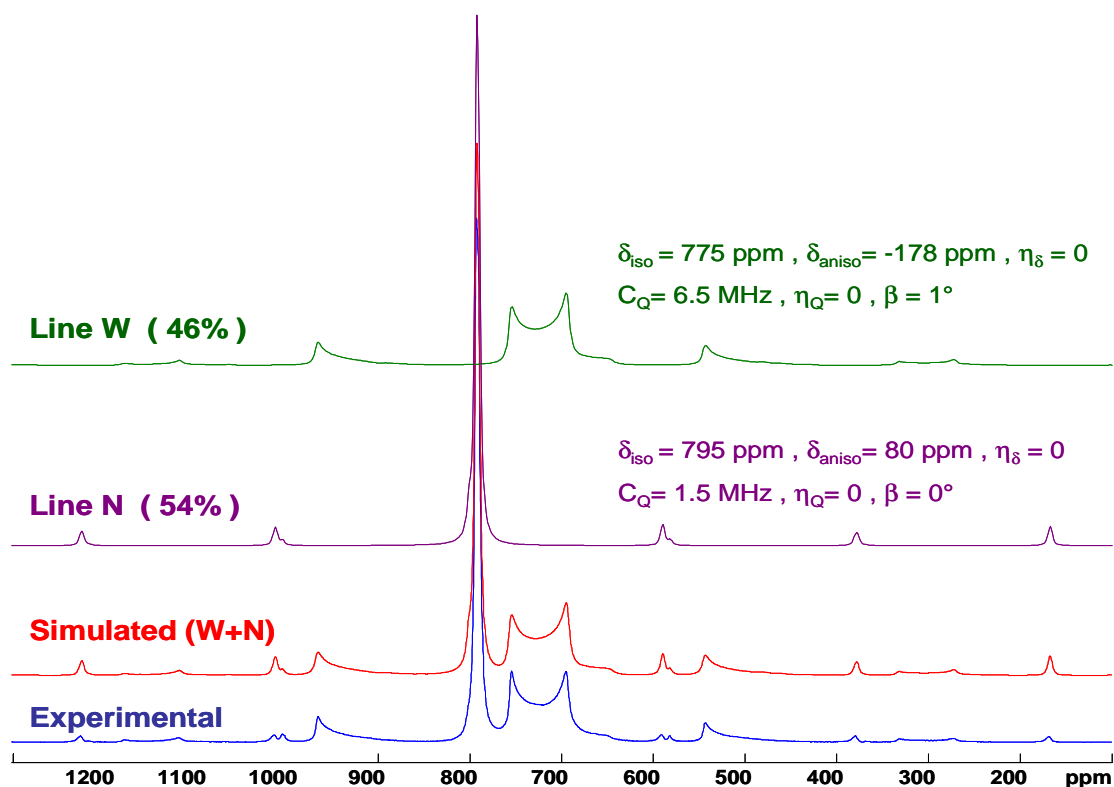


**Figure S7.** Spectral decomposition of the  $^{65}\text{Cu}$  full shifted echo NMR spectrum of the VS-CZTS compound acquired under MAS condition (30 kHz) on a 500 MHz spectrometer (11.75 T).

## References

- (1) Massiot, D.; Fayon, F.; Capron, M.; King, I.; Le Calvé, S.; Alonso, B.; Durand, J.-O.; Bujoli, B.; Gan, Z.; Hoatson, G. *Magnetic Resonance in Chemistry* **2002**, *40*, 70–76.
- (2) Kresse, G.; Furthmüller, J. *Phys. Rev. B* **1996**, *54*, 11169–11186.
- (3) Perdew, J.; Burke, K.; Ernzerhof, M. *Phys. Rev. Lett.* **1996**, *77*, 3865–3868.
- (4) Petrilli, H. M.; Blöchl, P. E.; Blaha, P.; Schwarz, K. *Phys. Rev. B* **1998**, *57*, 14690-14697.
- (5) Monkhorst, H. J.; Pack, J. D. *Phys. Rev. B* **1976**, *13*, 5188–5192.
- (6) Harris, R. K.; Becker, E. D.; De Menezes, S. M. C.; Goodfellow, R.; Granger, P. *Pure and Applied Chemistry* **2001**, *73*, 1795–1818.
- (7) Choubrac, L.; Lafond, A.; Guillot-Deudon, C.; Moëlo, Y.; Jolic, S. *Inorg. Chem.* **2012**, *51*, 3346–3348.
- (8) Pietrass, T.; Taulelle, F. *Magn. Reson. Chem.* 1997, *35*, 363–366.
- (9) Bastow, T. J.; Stuart, S. N. *Phys. Status Solidi B* 1988, *145*, 719–728.